DMD Fast Forward. Published on July 23, 2009 as doi:10.1124/dmd.109.027193

Construction of triple transfected cells (OATP1B1/MRP2/MRP3 and OATP1B1/MRP2/MRP4) for analysis of the sinusoidal function of MRP3 and MRP4.

Masakazu Hirouchi, Hiroyuki Kusuhara, Reiko Onuki, Brian W. Ogilvie, Andrew Parkinson and Yuichi Sugiyama

Department of Molecular Pharmacokinetics, Graduate School of Pharmaceutical Sciences, The University of Tokyo, Hongo, Bunkyo-ku, Tokyo , Japan (M.H., H.K., R.O., Y.S.) ,

XenoTech, LLC, Lenexa, Kansas (B.W.O., A.P.)

DMD Fast Forward. Published on July 23, 2009 as DOI: 10.1124/dmd.109.027193
This article has not been copyedited and formatted. The final version may differ from this version.

Running title: Effect of sinusoidal efflux on the transcellular transport

Corresponding author: Yuichi Sugiyama Ph.D.
Laboratory of Molecular Pharmacokinetics, Graduate School of Pharmaceutical Sciences,
The University of Tokyo,
7-3-1 Hongo, Bunkyo-ku, Tokyo
113-0033, Japan.
Phone: +81-3-5841-4770;
Fax: +81-3-5841-4767;
E-mail: sugiyama@mol.f.u-tokyo.ac.jp

The number of text pages : 32
The number of tables : 2
The number of figures : 6
The number of references : 44
The number of words in Abstract : 250
The number of words in Introduction : 767
The number of words in Discussion : 1351

Abberviations

ABC ATP-binding cassette; AUC, area under the curve; Bis-AG, bispheol-A glucuronide; $E_2$17βG 17β-estradiol-17β-D-glucuronide; E3040G, 6-hydroxy-5,7-dimethyl-2-methylamino-4-(3-pyridymethyl)benzothiazole glucuronide; Gem-G; gemfibrozil 1-*O*-β-glucuronide; TGZ-G troglitazone glucuronide; HEK, human embryonic kidney; HPLC, high-performance liquid chromatography; LC/MS, liquid chromatography-mass spectrometry; MDCK, Madin-Darby Canine Kidney; MRP, multidrug resistance-associated protein; 4-MUG, 4-methylumbelliferone glucuronide; OATP organic anion transporting polypeptide;

DMD Fast Forward. Published on July 23, 2009 as DOI: 10.1124/dmd.109.027193
This article has not been copyedited and formatted. The final version may differ from this version.

Abstract

MRP3/*ABCC3* and MRP4/*ABCC4* are ABC transporters expressed in the sinusoidal membrane of hepatocytes. The purpose of the present study was to establish OATP1B1/MRP2/MRP3 and OATP1B1/MRP2/MRP4 triple transfectants as *in vitro* model of the hepatobiliary transport of anionic drugs. In order to find *in vivo* relevant Mrp3 probes, wild-type and *Mrp3*$^{-/-}$ mice were given gemfibrozil, E3040, troglitazone, bisphenol A and 4-methylumbelliferone orally. Plasma concentrations of the glucuronide conjugates were significantly lower in *Mrp3*$^{-/-}$ mice than wild-type mice. The systemic exposure of gemfibrozil, E3040, and troglitazone were similar in wild-type and *Mrp3*$^{-/-}$ mice. 4-Methylumbelliferone and bisphenol A was undetectable in the plasma. In MRP3-expressing membrane vesicles, ATP-dependent uptake of the glucuronide conjugates of estradiol, gemfibrozil, E3040 and troglitazone was markedly greater than in control, while MRP4-expressing membrane vesicles exhibited a significant ATP-dependent uptake of gemfibrozil glucuronide and estradiol glucuronide. MRP3 or MRP4 was expressed in the OATP1B1/MRP2 double transfectants using adenovirus. The expression levels of OATP1B1 and MRP2 proteins were maintained both in the OATP1B1/MRP2/MRP3 and OATP1B1/MRP2/MRP4 triple transfectants, where MRP3 and MRP4 were localized in the basal membrane. Significant reduction in the basal-to-apical flux of the glucuronide conjugates of estradiol, gemfibrozil, E3040 and troglitazone were observed in the OATP1B1/MRP2/MRP3 triple transfectants compared with the double transfectants, while significant reduction was observed only for gemfibrozil- and estradiol glucuronide in the OATP1B1/MRP2/MRP4 triple transfectants. These results suggest that MRP3- or MRP4-triple transfectants provide a simple and useful *in vitro* system for evaluating their importance in the hepatobiliary transport of drugs.

Introduction

One of the major functions of the liver is the removal of various endogenous and exogenous compounds from the blood circulation. This clearance process involves uptake across the basolateral membrane and excretion across the bile canalicular membrane. In addition, sinusoidal efflux is an essential function to prevent the intracellular accumulation of potentially toxic endobiotic and xenobiotic substances and their metabolites in the liver. For instance, glucuronide conjugates are mainly produced in the liver and undergo both sinusoidal efflux followed by urinary excretion and biliary excretion (Klaassen and Watkins, 1984; Suzuki and Sugiyama, 1998). The elimination pathways of the glucuronide conjugates are determined by the transport activities for the canalicular and sinusoidal efflux.

The molecular mechanism of the biliary excretion of many anionic compounds has been well characterized (Gerloff et al., 1998; Suzuki and Sugiyama, 1998; Keppler and Konig, 2000). It is generally accepted that multidrug resistance-associated protein 2 (MRP2/*ABCC2*) is responsible for the biliary excretion of various organic anions including glucuronide conjugates (Suzuki and Sugiyama, 1998; Konig et al., 1999a; Keppler and Konig, 2000). The importance of MRP2 in the disposition of organic anions has been highlighted by the fact that the biliary excretion of MRP2 substrates is almost completely abolished in MRP2-deficient mutant rats (Buchler et al., 1996; Paulusma et al., 1996). On the other hand, the molecular mechanism governing sinusoidal efflux is now being gradually clarified. Multidrug resistance-associated protein 3 (MRP3/*ABCC3*) accepts glucuronide and glutathione conjugates, as well as monovalent (e.g., taurocholate and glycocholate) and sulfated bile salts as substrate (Hirohashi et al., 2000; Akita et al., 2002a). In MRP2-deficient mutant rats, Mrp3 is upregulated at the sinusoidal membrane in the liver, to maintain hepatocellular

DMD Fast Forward. Published on July 23, 2009 as DOI: 10.1124/dmd.109.027193
This article has not been copyedited and formatted. The final version may differ from this version.

homeostasis by pumping into the blood stream those endo- and xenobiotics that cannot be excreted into bile. Akita et al. (2001, 2002b) have demonstrated that the sinusoidal efflux of taurocholate correlated well with Mrp3 expression in rats (Akita et al., 2001; Akita et al., 2002b). Recently, the role of MRP3 as a basolateral efflux system has been explored in mice lacking Mrp3 (*Mrp3*$^{-/-}$ mice). *In vivo* and *in situ* studies using *Mrp3*$^{-/-}$ mice have demonstrated that Mrp3 plays a key role in the hepatic sinusoidal efflux of several glucuronide and sulfate conjugates (Manautou et al., 2005; Zelcer et al., 2005; Zamek-Gliszczynski et al., 2006; Zelcer et al., 2006) and that, under cholestatic conditions, Mrp3 also transports endogenous metabolites, such as bilirubin glucuronide and bile acid glucuronides (Belinsky et al., 2005; Zelcer et al., 2006). Another sinusoidal efflux transporter, multidrug resistance-associated protein 4 (MRP4/*ABCC4*) accepts a broad range of structurally diverse organic anions including several glucuronide and sulfate conjugates, as well as mono-anionic bile salts (Kruh and Belinsky, 2003; Rius et al., 2003; Zelcer et al., 2003; Ci et al., 2007; Hasegawa et al., 2007; Imaoka et al., 2007). Using *Abcc4*$^{-/-}$ mice, Zamek-Gliszczynski et al. (2006) demonstrated Mrp4 mediates the basolateral efflux of sulfate conjugates, while Mrp4 did not appear to play a major role in the transport of glucuronide conjugates (Zamek-Gliszczynski et al., 2006).

The double transfected Madin-Darby canine kidney II (MDCK II) cell lines expressing both human organic anion-transporting polypeptide 1B1 (OATP1B1/*SLCO1B1*) or OATP1B3 (*SLCO1B3*) in the basolateral membrane and canalicular ABC transporters, such as MRP2, P-glycoprotein (P-gp) and breast cancer resistance protein, in the apical membrane, have been established as an *in vitro* model of hepatic vectorial transport of organic anions in humans (Cui et al., 2001; Sasaki et al., 2002; Matsushima et al., 2005). Furthermore, Kopplow et al. constructed a quadruple-transfectants expressing three sinusoidal uptake transporters, OATP1B1, OATP1B3 and OATP2B1 in the basal

membrane and MRP2 in the apical membrane (Kopplow et al., 2005). It was clearly shown in monolayers of these double- and quadruple transfectants that many substrates are vectorially transported in the basal to the apical direction. However this model does not express sinusoidal efflux transporters, such as MRP3 and MRP4. Since the sinusoidal efflux transporters are now known to be one of the most important factors in governing the route of elimination of compounds from the liver and rate-limiting step of the hepatic elimination, there is a compelling need to establish an *in vitro* system that takes sinusoidal efflux into consideration.

In the present study, using *Mrp3*$^{-/-}$ mice, we demonstrated the importance of Mrp3 in the efflux of the glucuronide conjugates into the blood circulation following oral administration of their parent compounds (Figure 1). We have constructed triple transfected MDCK II cells, which express MRP3 or MRP4 at the basal membrane of OATP1B1/MRP2 double transfectants, and determined the transcellular transport of the glucuronide conjugates in the double- and triple transfectants.

DMD Fast Forward. Published on July 23, 2009 as DOI: 10.1124/dmd.109.027193
This article has not been copyedited and formatted. The final version may differ from this version.

Materials and methods

Materials

Gemfibrozil 1-*O*-β-glucuronide (Gem-G) was prepared by XenoTech, LLC (Lenexa, KS) as described below. E3040 and its glucuronide conjugate (E3040G) were kindly donated by Eisai. Co. Ltd. (Tokyo, Japan). Troglitazone and its glucuronide conjugate (TGZ-G) were kindly donated by Sankyo Co. (Tokyo, Japan). Bisphenol A glucuronide (Bis-AG) was kindly provided by Dr. Hiroshi Yokota (Rakuno Gakuen University, Hokkaido, Japan). [^{3}H]$E_2$17βG (51 Ci/mmol) with a purity of 98.5 % was purchased from New England Nuclear (Boston, MA). ATP, creatine phosphate and creatine phosphokinase were purchased from Sigma Chemical. Monoclonal antibody against MRP2 (M_2III6) and MRP4 (M4I-10) were purchased from Alexis Biochemicals (Gruenberg, Germany) and Abcam (Cambridge, UK), respectively and anti-OATP1B1 polyclonal antibody was from Alpha Diagnostic International Inc. (San Antonio, TX). Anti-MRP3 rabbit serum was produced, previously (Akita et al., 2002a). All other chemicals used were commercially available and of reagent grade.

Preparation of gemfibrozil glucuronide

Gem-G was biosynthesized in vitro with dog liver microsomes. The incubation mixtures (40 x 2 mL) contained dog liver microsomes (2 mg/mL), the zwitterionic detergent 3-[(3-cholamidopropyl)dimethylammonio]-1-propanesulfonate (CHAPS; 10 mM), Tris-HCl (100 mM, pH 7.7 at 37°C), EDTA (2.0 mM), $MgCl_2$ (10 mM), D-saccharic acid 1,4-lactone (100 µM), UDP-glucuronic acid (8.0 mM) and gemfibrozil (4 mM). Incubations were carried out for 8 hours at 37°C and were stopped by the addition of 60% perchloric acid (w/v) (final concentration of approximately 1.5% v/v). The acidified samples were extracted with ethyl acetate (2 x 4 mL). The

organic extracts were pooled, evaporated in a vacuum centrifuge and reconstituted in 50% acetonitrile/water containing (v/v) 1% formic acid (v/v). After insoluble material was removed by centrifugation, aliquots (400 µL) of the reconstituted samples were subjected to HPLC on a Supelcosil LC-18, 4.6x150 mm column. Gem-G was separated from gemfibrozil with a linear gradient mixture of water and acetonitrile, each of which contained 0.1% formic acid, at a flow rate of 1 mL/min. Gem-G was monitored by fluorescence (λem: 284 nm, λem: 316 nm) and UV detection (235 nm) and its identity was confirmed by comparison with a standard that had been characterized by LC/MS/MS and NMR (prepared and characterized as described previously (Ogilvie et al., 2006)). The Gem-G fractions were collected (retention time 6-8 min) and lyophilized. The white solid (approximately 100 mg) was transferred to amber vials and stored desiccated at –20ºC.

Animals

Male *Mrp3*$^{-/-}$ mice and wild type FVB mice (12 – 18 weeks) were used in this study. They are fertile and do not exhibit any obvious physiological abnormalities. *Mrp3*$^{-/-}$ mice used in this study have been described previously (Zelcer et al., 2006). All animals were treated humanely and all experiments were reviewed and approved by the Institutional Animal Care Committee (Graduate School of Pharmaceutical Sciences, The University of Tokyo).

Determination of plasma pharmacokinetics of glucuronide conjugates in wild-type and *Mrp3*$^{-/-}$ mice

Mice were given oral doses of gemfibrozil (20 mg/kg), E3040 (2 mg/kg), troglitazone (25 mg/kg), bisphenol A (10 mg/kg) and 4-methylumbelliferon (18 mg/kg). Blood samples were collected

from the tail artery 10, 20, 30, 60, 120 and 180 min after administration and an aliquot (8 µl) of each sample was mixed with 16 µl acetonitrile. After the precipitated protein was removed by centrifugation, an aliquot (20 µl) of the supernatant fraction was diluted with 80 µl Milli-Q and 30-µl aliquots were analyzed by Liquid Chromatography/Mass Spectrometry (LC/MS) as described below.

Construction of recombinant adenoviruses containing MRP3 and MRP4

Human MRP3 and MRP4 cDNAs used in this study were cloned previously (Kiuchi et al., 1998; Hasegawa et al., 2007). The MRP3 and MRP4 cDNAs were initially subcloned into the Apa I and Kpn I sites of the p shuttle, which has I-Ceu I and PI-Sce I sites upstream and downstream of the MRP3 and MRP4 expression cassettes, respectively. The I-CeuI / PI-SceI digested fragments of p shuttle-MRP3 and MRP4 were ligated with I-CeuI / PI-SceI digested Adeno-X^{TM} Viral DNA (BD Biosciences, Palo Alto, CA), resulting in pAd-MRP3 and pAd-MRP4. To generate the recombinant viruses, both pAd-MRP3 and pAd-MRP4 were digested with PacI. Linearized DNAs were transfected into HEK293 cells grown in a 12-well dish with Fugene 6 (Roche Diagnostics Corp.) according to the manufacturer's instructions. Viruses (Ad-MRP3 and Ad-MRP4) were prepared as described previously (Mizuguchi and Kay, 1998). Recombinant viruses were purified by CsCl gradient centrifugation, dialyzed with a solution containing 10 mM Tris (pH 7.5), 1 mM $MgCl_2$ and 10% glycerol and aliquots stored at -80 °C. The resulting virus titer was determined as described previously (Mizuguchi and Kay, 1999).

Preparation of membrane vesicles of MRP3 and MRP4

HEK293 cells cultured in a 15cm dish were infected by recombinant adenoviruses containing

DMD Fast Forward. Published on July 23, 2009 as DOI: 10.1124/dmd.109.027193
This article has not been copyedited and formatted. The final version may differ from this version.

MRP3 (10 MOI) and MRP4 (10 MOI). As a negative control, cells were infected with Ad-tTA (10 MOI). Cells were harvested 48 h after infection and then the membrane vesicles were isolated from 1-2 $x10^8$ cells as described in detail previously (Hasegawa et al., 2007). Briefly, cells were diluted 40-fold with hypotonic buffer (1 mM Tris-HCl, 0.1 mM EDTA, pH 7.4, at 4 °C) and stirred gently for 1 hr on ice in the presence of 2 mM phenylmethylsulfonyl fluoride, 5 µg/ml leupeptin, 1 µg/ml pepstatin and 5 µg/ml aprotinin. The cell lysate was centrifuged at 100,000 g for 30 min at 4 °C and the resulting pellet was suspended in 10 ml isotonic TS buffer (10 mM Tris-HCl, 250 mM sucrose, pH 7.4 at 4 °C) and homogenized with a Dounce B homogenizer (glass/glass, tight pestle, 30 strokes). The crude membrane fraction was layered on top of a 38% (w/v) sucrose solution in 5 mM Tris-HEPES, pH 7.4 at 4 °C and centrifuged in a Beckman SW41 rotor centrifuge at 280,000 g for 45 min at 4 °C. The turbid layer at the interface of the sucrose cushion was collected, diluted to 23 ml with TS buffer and centrifuged at 100,000 g for 30 min at 4 °C. The resulting pellet was suspended in 400 µl TS buffer. Vesicles were formed by passing the suspension 30 times through a 27-gauge needle using a syringe. Control and MRP2-expressing LLC-PK1 membrane vesicles were prepared as previously reported (Hirouchi et al., 2004). The membrane vesicles were finally frozen in liquid nitrogen and stored at –80 °C until use. Protein concentrations were determined by the method of Lowry.

Determination of ATP-dependent uptake by membrane vesicle expressing MRP2, MRP3 and MRP4.

The uptake study of Gem-G (25 µM), E3040G (0.5 µM), TGZ-G (10 µM) and [^{3}H] $E_2$17βG (0.3 µM) was performed as reported previously (Hirohashi et al., 2000; Hasegawa et al., 2007).

DMD Fast Forward. Published on July 23, 2009 as DOI: 10.1124/dmd.109.027193
This article has not been copyedited and formatted. The final version may differ from this version.

Briefly, the transport medium (10 mM Tris, 250 mM sucrose and 10 mM $MgCl_2$, pH 7.4 at 37 °C) contained the ligands (the glucuronide conjugates), 5 mM ATP and an ATP-regenerating system consisting of 10 mM creatine phosphate and 100 µg/µl creatine phosphokinase. An aliquot of transport medium (17-18 µl) was mixed rapidly with the vesicle suspension (10 µg protein in 2-3 µl) and the transport reaction was stopped by the addition of 1 ml of ice-cold buffer containing 250 mM sucrose, 0.1 M NaCl and 10 mM Tris-HCl (pH 7.4 at 4 °C). The stopped reaction mixture was passed through a 0.45 µm HA filter (Millipore Corp., Bedford, MA) and then washed twice with 5 ml stop solution. The radioactivity of [^{3}H] $E_2$17βG retained on the filter was measured in a liquid scintillation counter (LS 6000SE, Beckman Instruments, Fullerton, CA) after the addition of scintillation cocktail (Clear-sol I, Nacalai Tesque, Tokyo, Japan). Non-radioactive substrates retained on the membrane filter (JH-filter, Milipore) were dissolved in 1 ml methanol containing internal standard using sonication for 15 min. After centrifugation, supernatants were concentrated and dissolved in 75 µl Milli-Q water and 50 µl aliquots were analyzed by LC/MS as described below. Ligand uptake was normalized to the amount of membrane protein.

Western blotting

For Western blotting, the isolated crude membranes were dissolved in 3x SDS sample buffer (New England BioLabs, Beverly, MA) and subjected to electrophoresis on an 8.5 % SDS-polyacrylamide gel with a 4.4% stacking gel. The molecular weight was determined with a prestained protein marker (New England BioLabs, Beverly, MA). Proteins were transferred electrophoretically to a nitrocellulose membrane (Millipore, Bedford, MA) with a trans-blotter (Bio-Rad Laboratories, Richmond, CA) at 15 V for 1 hr. Non-specific binding on the membrane were

blocked with 2.5% skimmed milk for 1 hr at room temperature, after which the membrane was incubated for 1 hr at room temperature in skimmed milk with a 1,000-fold dilution of anti-OATP1B1 polyclonal antibody, a 200-fold dilution of monoclonal antibody against MRP2 (M_2III6), a 1000-fold dilution of anti-MRP3 rabbit serum and a 200-fold dilution of anti-MRP4 monoclonal antibody (M4I-10). For the detection of each transporter, the membrane was incubated with a 2,500-fold diluted donkey anti-rabbit (OATP1B1 and MRP3), anti-mouse IgG (MRP2) and anti-rat IgG (MRP4) conjugated with horseradish peroxidase (Amersham Biosciences Inc., Piscataway, NJ) for 1hr in skimmed milk. The immunoreactive band was detected with an ECL Plus Western blotting starter kit (Amersham Biosciences) and its intensity was quantified in a luminescent image analyzer (LAS-3000mini; Fuji Film Corp., Tokyo, Japan).

Immunohistochemical staining of MRP3 and MRP4

For the immunohistochemical staining, MDCK II cells were grown in 12-well dishes. Recombinant adenoviruses containing MRP3 (150 MOI) or MRP4 (150 MOI) were infected 48 hr prior to starting the experiments. After fixation with ice-cold methanol for 10 min and permeabilization in 1% Triton X-100 in phosphate-buffered saline for 10 min, cells were incubated with a 40-fold dilution of monoclonal antibody against MRP2 (M_2III6), a 200-fold dilution of anti-MRP3 rabbit serum, or a 50-fold dilution of monoclonal antibody against MRP4 (M4I-10) for 1 hr at room temperature. Then, cells were washed three times with phosphate-buffered saline and incubated for 1 hr at room temperature with a 250-fold dilution of goat anti-mouse IgG Alexa 568 (Molecular Probes Inc., Eugene, OR) for MRP2, goat anti-rabbit IgG Alexa 488 for MRP3 and goat anti-rat IgG Alexa 488 for MRP4. Nuclei were stained with 250-fold diluted TO-PRO-3 iodide

(Molecular Probes Inc.). The localization of each protein was visualized by confocal laser microscopy (Zeiss LSM-510; Carl Zeiss Inc., Thornwood, NY).

Determination of the transcellular transport of glucuronide conjugates

The OATP1B1/MRP2 double transfectants used in this study was established previously (Sasaki et al., 2002). The transcellular transport studies were performed as reported previously (Sasaki et al., 2002). Briefly, MDCKII cells were grown on Transwell membrane inserts (6.5 mm diameter, 0.4 μm pore size; Corning Coster, Bodenheim, Germany) at confluence for 3 days and infected with MRP3 or MRP4 recombinant adenovirus (150 MOI). The expression of OATP1B1 and MRP2 was induced with 5 mM sodium butyrate for 48 hr. Cells were first washed with Krebs-Henseleit buffer (142 mM NaCl, 23.8 mM $NaHCO_3$, 4.83 mM KCl, 0.96 mM KH_2PO_4, 1.20 mM $MgSO_4$, 12.5 mM HEPES, 5 mM glucose and 1.53 mM $CaCl_2$ to pH 7.3) at 37 °C then substrates were added in Krebs-Henseleit buffer to either the apical compartment (250μl) or the basolateral compartment (1ml). After the designated times, the substrate concentration in the opposite compartment was measured by LC/MS as described below. At the end of the experiments, the cells were washed three times with 1.5 ml ice-cold Krebs-Henseleit buffer and solubilized in 500 μl 0.2 M NaOH. After addition of 100 μl 1 M HCl, 50 μl aliquots of cell lysate were used to determine protein concentrations by the method of Lowry with bovine serum albumin as a standard.

Liquid chromatography/mass spectrometry conditions

Non-radioactive substrates were all quantified by HPLC (Alliance 2690, Waters, Milford, MA, USA) connected to a mass spectrometer (ZQ, Micromass, Manchester, UK). Detailed LC conditions

and mass-to-charge ratios are shown in Table 1.

Statistical analysis

Statistical analysis was performed by Student's t-test to identify significant differences between pairs of data sets.

DMD Fast Forward. Published on July 23, 2009 as DOI: 10.1124/dmd.109.027193
This article has not been copyedited and formatted. The final version may differ from this version.

Results

Plasma concentrations of glucuronide conjugates in *Mrp3*$^{-/-}$ mice following oral administration of the parent compounds

To find in vivo relevant probes for Mrp3, in vivo experiments using *Mrp3*$^{-/-}$ mice were performed. Wild-type and *Mrp3*$^{-/-}$ mice were given gemfibrozil, E3040, troglitazone, bisphenol A, 4-methylumbelliferon orally, and the plasma concentrations of their glucuronide conjugates were determined (Figure 2). Mrp3 dysfunction resulted in a much lower plasma concentration of all glucuronide conjugates compared to wild-type mice (Figure 2) whereas the area under the plasma concentration time curve (AUC) of the parent drugs tested was not statistically different between wild-type and *Mrp3*$^{-/-}$ mice except bisphenol A and 4-methylumbelliferon (Table 2). Plasma concentrations of bisphenol A and 4-methylumbelliferon were below the limit of the detection both in wild-type and *Mrp3*$^{-/-}$ mice.

ATP-dependent uptake of glucuronide conjugates in membrane vesicles

To confirm the transport activities of Gem-G, E3040G and TGZ-G by MRP2, MRP3 and MRP4, the uptake of the glucuronide conjugates was determined in mock, MRP2-, MRP3- or MRP4-expressing membrane vesicles in the presence of ATP and AMP by rapid filtration method. $E_2$17βG was used as a positive control because this compound is well known to be a common substrate for MRP2, MRP3 and MRP4 (Suzuki and Sugiyama, 1998; Chen et al., 2001; Akita et al., 2002a).

The ATP-dependent uptake of all the glucuronide conjugates at 2 min was significantly higher in MRP2-expressing membrane vesicles compared with control membrane vesicles (Figure 3). The

DMD Fast Forward. Published on July 23, 2009 as DOI: 10.1124/dmd.109.027193
This article has not been copyedited and formatted. The final version may differ from this version.

ATP-dependent uptake of all the glucuronide conjugates at 2 min was also significantly higher in MRP3-expressing membrane vesicles compared with control membrane vesicles (Figure 3), while only Gem-G and $E_2$17βG exhibited statistical significance in the ATP-dependent uptake by MRP4 expressing membrane vesicles compared with that in control vesicles.

Expression and membrane localization of MRP3 and MRP4 in MDCK II cells.

The expression level of OATP1B1, MRP2 and MRP3 or MRP4 proteins was confirmed by Western blotting (Figure 4). OATP1B1 and MRP2 proteins were detected in the OATP1B1/MRP2 double, and OATP1B1/MRP2/MRP3 and OATP1B1/MRP2/MRP4 triple transfectants. Semiquantitative analysis of the results showed that the expression levels of OATP1B1 and MRP2 in the triple transfected MDCK II cells were about the same as those in the OATP1B1/MRP2 double transfectants. The signals for MRP3 or MRP4 could only be detected in the triple transfected MDCK II cells, showing the specificity of the antibody.

The expression levels of MRP3 and MRP4 protein in the triple transfectants were compared with those in human liver by Western blotting (Figure 4). Three bands were detected in human liver by anti-MRP3 antibody for an unknown reason (Figure 4a), and the band density of the major band (the middle band) was compared with that in the triple transfectants in terms of the intensity and molecular weight. Semiquantitative analysis showed that the band densities were comparable between human liver and the MRP3 triple transfectant. In the case of MRP4, the frontline of the bands detected by anti-MRP4 antibody was similar between human liver and OATP1B1/MRP2/MRP4 triple transfectant. However, the band density was markedly lower in the human liver compared with that in the MRP4 triple transfectant (Figure 4b).

DMD Fast Forward. Published on July 23, 2009 as DOI: 10.1124/dmd.109.027193
This article has not been copyedited and formatted. The final version may differ from this version.

Double immunostaining of MRP3 or MRP4 with MRP2 was performed to show membrane localization of MRP3 and MRP4 in MDCK II cells. MRP2 is predominantly localized in the apical membrane of MDCK II cells as reported previously (Evers et al., 1998; Cui et al., 1999; Sasaki et al., 2002). The signals associated with MRP3 were detected both in the cytoplasmic area and basal membrane, but did not show any overlap with those associated with MRP2 (Figure 5a). The membrane localization of MRP3 and MRP4 was consistent with previous reports (Konig et al., 1999b; Lai and Tan, 2002). The signals associated with MRP4 were predominantly localized on the basolateral membrane of the double transfected MDCK II cells, and did not show any overlap with MRP2 signals (Figure 5b).

Transcellular transport of the glucuronide conjugates across MDCK II monolayers

Basal-to-apical and apical-to-basal transcellular transport of Gem-G, $E_2$17βG, E3040G and TGZ-G across the monolayers was determined in mock control, OATP1B1/MRP2 double- and OATP1B1/MRP2/MRP3 and OATP1B1/MRP2/MRP4 triple transfectants. The experiments were performed three times in triplex to confirm reproducibility. Figure 6 shows the representative data. Compared to mock control, expression of OATP1B1 and MRP2 greatly enhanced the basal-to-apical transport of Gem-G, $E_2$17βG, E3040G and TGZ-G. 4MUG did not show a directional transcellular transport (data not shown). In the subsequent studies, Gem-G, $E_2$17βG, E3040G and TGZ-G were used as test compounds. The basal-to-apical flux of the glucuronide conjugates was significantly greater than the apical-to-basal flux in the OATP1B1/MRP2/MRP3 triple transfectants. However, the basal-to-apical flux of $E_2$17βG, Gem-G, E3040G and TGZ-G in the OATP1B1/MRP2/MRP3 triple transfectant was significantly lower than that in OATP1B1/MRP2 double transfectants, 69, 77, 66 and

DMD Fast Forward. Published on July 23, 2009 as DOI: 10.1124/dmd.109.027193
This article has not been copyedited and formatted. The final version may differ from this version.

43% of the double transfectant. The directional transport of the glucuronide conjugates in the basal-to-apical direction was also maintained in the OATP1B1/MRP2/MRP4 triple transfectants. However, the basal-to-apical flux was significantly lower in the OATP1B1/MRP2/MRP4 triple transfectants only for of $E_2$17βG and Gem-G compared with that in OATP1B1/MRP2 double transfectant, 78 and 64% of the double transfectant, respectively. Expression of MRP4 did not affect the basal-to-apical flux of E3040G and TGZ-G (Figure 6c and d). Since the apical-to-basal transport of the glucuronide conjugates was similar between the double and triple transfectants, adenovirus infection and butylate treatment did not induce non-specific transport.

DMD Fast Forward. Published on July 23, 2009 as DOI: 10.1124/dmd.109.027193
This article has not been copyedited and formatted. The final version may differ from this version.

Discussion

MRP3- and MRP4-mediate the efflux of drugs and their metabolites into the blood circulation in the sinusoidal membrane of hepatocytes, and competes with canalicular efflux and metabolism in the liver for their common substrates. In the present study, we constructed triple transfected MDCK II cells that express OATP1B1, MRP2 and either MRP3 or MRP4, as in vitro model for hepatobiliary transport of organic anions in humans, and examined the effect of the expression MRP3 or MRP4 on the directional transcellular transport of their substrate compounds in the basal-to-apical direction by OATP1B1 and MRP2.

Mrp3$^{-/-}$ mice have provided information about the role of hepatic Mrp3 in the disposition of several glucuronide conjugates and methotrexate (Manautou et al., 2005; Zelcer et al., 2005; Zamek-Gliszczynski et al., 2006; Zelcer et al., 2006). In order to identify some probe compounds for sinusoidal efflux analysis, we examined the *in vivo* disposition of five glucuronide conjugates, namely Gem-G, E3040G, TGZ-G, Bis-AG and 4-MUG in wild-type and *Mrp3*$^{-/-}$ mice. Mrp3 dysfunction caused a marked reduction in the plasma concentration of these glucuronide conjugates following oral administration of their parent compounds suggesting that Mrp3 plays a key role in the efflux of these glucuronide conjugates into the systemic circulation. This is in a good agreement with previous findings (Manautou et al., 2005; Zelcer et al., 2005; Zamek-Gliszczynski et al., 2006; Zelcer et al., 2006). It should be noted that Mrp3 in the enterocytes could contribute to the differences in plasma levels of the glucuronide conjugates determined in addition to Mrp3 in the liver since the parent drugs were given orally, and glucuronidation also occurs in the small intestine (Grams et al., 2000) where Mrp3 is expressed in the basolateral membrane (Rost et al., 2002; Shoji et al., 2004; Zelcer et al., 2006).

DMD Fast Forward. Published on July 23, 2009 as DOI: 10.1124/dmd.109.027193
This article has not been copyedited and formatted. The final version may differ from this version.

In vivo study using *Mrp3*$^{-/-}$ mice showed that the glucuronide conjugates are in vivo relevant probes for MRP3. To examine species difference in the substrate recognition/transport activities between mouse and human MRP3, in vitro transport studies using membrane vesicles were carried out to confirm that the glucuronide conjugates are substrates of MRP2, MRP3 and MRP4. Both MRP2 and MRP3-expressing membrane vesicles exhibited a significantly higher ATP-dependent accumulation of Gem-G E3040G and TGZ-G as well as $E_2$17βG compared with mock control (Figure 3). It was confirmed that the glucuronide conjugates, in the disposition of which Mrp3 is deeply involved (Figure 2), are MRP3 substrates, excluding a remarkable species difference in the substrate recognition/transport activity by mouse and human MRP3 as far as these glucuronide conjugates are concerned. Unlike MRP2 and MRP3, only $E_2$17βG and Gem-G exhibited a significant ATP-dependent uptake in MRP4-expressing membrane vesicles that was statistically significant, indicating that E3040G and TGZ-G are poor MRP4 substrates. It should be noted that, for quantitative interpretation of the results, the uptake under liner conditions must be compared. As for E3040G, which exhibited a striking difference between MRP3 and MRP4, its K_i value for MRP3 was reported to be 5.6 μM (Akita et al., 2002a), and that for MRP4 was 27.9μM (unpublished data by Takeuchi, Kusuhara and Sugiyama). These values were considerably greater than the concentration in the incubating buffer (0.5μM). Absence of significant ATP-dependent uptake of E3040G in MRP4 expressing membrane vesicles compared with control vesicles is not due to saturation.

We previously constructed MDCK II cells that express both human OATP1B1 and MRP2 which greatly enhance the transcellular transport of their common substrates, generally amphipathic anionic drugs in the basal-to-apical direction (Sasaki et al., 2002). In the present study, we have constructed the triple transfectant expressing either MRP3 or MRP4 by infection of adenovirus

DMD Fast Forward. Published on July 23, 2009 as DOI: 10.1124/dmd.109.027193
This article has not been copyedited and formatted. The final version may differ from this version.

containing MRP3 or MRP4 cDNA to the OATP1B1/MRP2 double transfectants. The expression of OATP1B1 and MRP2 proteins was maintained in the OATP1B1/MRP2/MRP3 and OATP1B1/MRP2/MRP4 triple transfectants (Figure 4). Immunofluorescence analysis by confocal laser microscopy showed that MRP3 was localized at the basal membrane as well as the cytoplasmic region in MDCK II cells (Figure 5a), while MRP4 was also localized at the basal membrane (Figure 5b). The membrane localization of MRP2, MRP3 and MRP4 is consistent with the results of a previous study (Evers et al., 1998; Cui et al., 1999; Konig et al., 1999b; Sasaki et al., 2002; Lai and Tan, 2002). Therefore, the basal-to-apical transport in the triple transfectants will become lower than that in the double transfectants when MRP3 or MRP4-mediated basolateral efflux is comparable or greater than the apical efflux mediated by MRP2. The basal-to-apical flux of Gem-G, $E_2$17βG, E3040G and TGZ-G in the OATP1B1/MRP2/MRP3 triple transfectant was significantly reduced compared with that in the OATP1B1/MRP2 double transfectant (Figure 6). In the OATP1B1/MRP2/MRP4 triple transfectant, only Gem-G and $E_2$17βG showed a significant reduction in the basal-to-apical flux compared with the OATP1B1/MRP2 double transfectant. MRP4 expression had no effect on the basal-to-apical transport of E3040G and TGZ-G. This is reasonable considering that E3040G and TGZ-G are poor MRP4 substrates (Figure 3). Therefore, the triple transfectants allow screening of MRP3 and MRP4 substrates with significant transport activities. Expression of MRP3 and MRP4 protein was compared between human liver specimens and the triple transfectants. Expression of MRP3 protein was similar between the human liver and OATP1B1/MRP2/MRP3 triple transfectants (Figure 4b). However, considering the cytosolic distribution of MRP3 as well as plasma membrane in MDCK II cells (Figure 5a), the actual amount of MRP3 protein involved in the efflux will be smaller in the triple transfectants compared with human liver. On the other hand, expression of MRP4 protein

is considerably higher in the OATP1B1/MRP2/MRP4 triple transfectants than in the human liver (Figure 4b), indicating that impact of MRP4 is overestimated in the triple transfectants. The triple transfectants have an advantage in the application of existing high throughput screening systems compared with membrane vesicles for the first screening. We have already constructed all combinations of the uptake and canalicular efflux transporters using MDCK II cells (Matsushima et al., 2005; Ishiguro et al., 2008). Infection of adenovirus containing MRP3 or MRP4 cDNA to other double transfectants will easily allow examination of any overlap of substrate specificities between sinusoidal and canalicular efflux transporters. However, it is evident that the triple transfectants cannot quantitatively predict in vivo impact of MRP3 and MRP4 on the hepatic elimination because of difference in protein expression between human liver and triple transfectants, and overlapped substrate specificities of MRP3 and MRP4. Actually, the impact of Mrp4 dysfunction on the plasma concentrations of the glucuronide conjugates of acetaminophen, 4-methylumbelliferone and harmol was negligible in mice, while Mrp3 dysfunction showed a great impact (Zamek-Gliszczynski et al., 2006). Further studies are necessary to establish a more quantitative method to predict the impact of MRP3 and MRP4-mediated sinusoidal efflux in the hepatobiliary transport.

The hepatobiliary elimination of amphipathic anionic drugs involves three membrane transport processes, uptake, sinusoidal and canalicular efflux. The rate-limiting step in the hepatic elimination must be taken into consideration when predicting the effect of functional changes in the metabolism and canalicular efflux caused by drug-drug interactions and genetic polymorphisms on the systemic exposure of drugs (Kusuhara and Sugiyama, 2009). In the case that sinusoidal efflux is markedly lower than the hepatic metabolism and canalicular efflux, the uptake process becomes the rate-limiting step of the net hepatic elimination from the systemic circulation. Under this condition, alteration of

activities of hepatic metabolism and canalicular efflux hardly affects the systemic exposure of drugs, while it greatly affects the liver concentration. Whether drugs are substrates of MRP3 and/or MRP4 with the transport activities comparable with metabolism and canalicular efflux is critical information for understanding the rate-limiting step in the hepatic elimination. Only a few studies have examined the rate-limiting process in hepatic elimination of drugs (Ueda et al., 2001; Kitamura et al., 2008; Watanabe et al., 2009). Transport studies using the triple transfectants will give clues about the rate-limiting process in hepatobiliary transport.

In conclusion, we have constructed MRP3 and MRP4 triple transfected MDCK II cell lines and demonstrated that the vectorial transport of several glucuronide conjugates is reduced compared with that of double transfectant cells. Our triple transfectants provide a useful and simple experimental system for predicting the significance of sinusoidal efflux in hepatobiliary transport.

Acknowledgement

We are grateful to Dr. Piet Borst (The Netherlands Cancer Institute, Amsterdam, The Netherlands) for supplying *Mrp3*$^{-/-}$ mice and to Phyllis Yerino (XenoTech) for her assistance in the preparation of gemfibrozil glucuronide.

References

Akita H, Suzuki H, Hirohashi T, Takikawa H and Sugiyama Y (2002a) Transport activity of human MRP3 expressed in Sf9 cells: comparative studies with rat MRP3. *Pharm Res* **19**:34-41.

Akita H, Suzuki H and Sugiyama Y (2001) Sinusoidal efflux of taurocholate is enhanced in Mrp2-deficient rat liver. *Pharm Res* **18**:1119-1125.

Akita H, Suzuki H and Sugiyama Y (2002b) Sinusoidal efflux of taurocholate correlates with the hepatic expression level of Mrp3. *Biochem Biophys Res Commun* **299**:681-687.

Belinsky MG, Dawson PA, Shchaveleva I, Bain LJ, Wang R, Ling V, Chen ZS, Grinberg A, Westphal H, Klein-Szanto A, Lerro A and Kruh GD (2005) Analysis of the in vivo functions of Mrp3. *Mol Pharmacol* **68**:160-168.

Buchler M, Konig J, Brom M, Kartenbeck J, Spring H, Horie T and Keppler D (1996) cDNA cloning of the hepatocyte canalicular isoform of the multidrug resistance protein, cMrp, reveals a novel conjugate export pump deficient in hyperbilirubinemic mutant rats. *J Biol Chem* **271**:15091-15098.

Chen ZS, Lee K and Kruh GD (2001) Transport of cyclic nucleotides and estradiol 17-beta-D-glucuronide by multidrug resistance protein 4. Resistance to 6-mercaptopurine and 6-thioguanine. *J Biol Chem* **276**:33747-33754.

Ci L, Kusuhara H, Adachi M, Schuetz JD, Takeuchi K and Sugiyama Y (2007) Involvement of MRP4 (ABCC4) in the luminal efflux of ceftizoxime and cefazolin in the kidney. *Mol Pharmacol* **71**:1591-1597.

Cui Y, Konig J, Buchholz JK, Spring H, Leier I and Keppler D (1999) Drug resistance and ATP-dependent conjugate transport mediated by the apical multidrug resistance protein, MRP2, permanently expressed in human and canine cells. *Mol Pharmacol* **55**:929-937.

Cui Y, Konig J, Leier I, Buchholz U and Keppler D (2001) Hepatic uptake of bilirubin and its conjugates by the human organic anion transporter SLC21A6. *J Biol Chem* **276**:9626-9630.

Evers R, Kool M, van Deemter L, Janssen H, Calafat J, Oomen LC, Paulusma CC, Oude Elferink RP, Baas F, Schinkel AH and Borst P (1998) Drug export activity of the human canalicular multispecific organic anion transporter in polarized kidney MDCK cells expressing cMOAT (MRP2) cDNA. *J Clin Invest* **101**:1310-1319.

Gerloff T, Stieger B, Hagenbuch B, Madon J, Landmann L, Roth J, Hofmann AF and Meier PJ (1998) The sister of P-glycoprotein represents the canalicular bile salt export pump of mammalian liver. *J Biol Chem* **273**:10046-10050.

Grams B, Harms A, Braun S, Strassburg CP, Manns MP and Obermayer-Straub P (2000) Distribution

and inducibility by 3-methylcholanthrene of family 1 UDP-glucuronosyltransferases in the rat gastrointestinal tract. *Arch Biochem Biophys* **377**:255-265.

Hasegawa M, Kusuhara H, Adachi M, Schuetz JD, Takeuchi K and Sugiyama Y (2007) Multidrug resistance-associated protein 4 is involved in the urinary excretion of hydrochlorothiazide and furosemide. *J Am Soc Nephrol* **18**:37-45.

Hirohashi T, Suzuki H, Chu XY, Tamai I, Tsuji A and Sugiyama Y (2000) Function and expression of multidrug resistance-associated protein family in human colon adenocarcinoma cells (Caco-2). *J Pharmacol Exp Ther* **292**:265-270.

Hirouchi M, Suzuki H and Sugiyama Y (2004) Characterization of the Cellular Localization, Expression Level, and Function of SNP Variants of MRP2/ABCC2. *Pharm Res* **12**:387-439.

Imaoka T, Kusuhara H, Adachi M, Schuetz JD, Takeuchi K and Sugiyama Y (2007) Functional involvement of multidrug resistance-associated protein 4 (MRP4/ABCC4) in the renal elimination of the antiviral drugs adefovir and tenofovir. *Mol Pharmacol* **71**:619-627.

Ishiguro N, Maeda K, Saito A, Kishimoto W, Matsushima S, Ebner T, Roth W, Igarashi T and Sugiyama Y (2008) Establishment of a set of double transfectants coexpressing organic anion transporting polypeptide 1B3 and hepatic efflux transporters for the characterization of the hepatobiliary transport of telmisartan acylglucuronide. *Drug Metab Dispos* **36**:796-805.

Keppler D and Konig J (2000) Hepatic secretion of conjugated drugs and endogenous substances. *Semin Liver Dis* **20**:265-272.

Kitamura Y, Hirouchi M, Kusuhara H, Schuetz JD and Sugiyama Y (2008) Increasing systemic exposure of methotrexate by active efflux mediated by multidrug resistance-associated protein 3 (mrp3/abcc3). *J Pharmacol Exp Ther* **327**:465-473.

Kiuchi Y, Suzuki H, Hirohashi T, Tyson CA and Sugiyama Y (1998) cDNA cloning and inducible expression of human multidrug resistance associated protein 3 (MRP3). *FEBS Lett* **433**:149-152.

Klaassen CD and Watkins JB, 3rd (1984) Mechanisms of bile formation, hepatic uptake, and biliary excretion. *Pharmacol Rev* **36**:1-67.

Konig J, Nies AT, Cui Y, Leier I and Keppler D (1999a) Conjugate export pumps of the multidrug resistance protein (MRP) family: localization, substrate specificity, and MRP2-mediated drug resistance. *Biochim Biophys Acta* **1461**:377-394.

Konig J, Rost D, Cui Y and Keppler D (1999b) Characterization of the human multidrug resistance protein isoform MRP3 localized to the basolateral hepatocyte membrane. *Hepatology* **29**:1156-1163.

Kopplow K, Letschert K, Konig J, Walter B and Keppler D (2005) Human hepatobiliary transport of organic anions analyzed by quadruple-transfected cells. *Mol Pharmacol* **68**:1031-1038.

Kruh GD and Belinsky MG (2003) The MRP family of drug efflux pumps. *Oncogene* **22**:7537-7552.

Kusuhara H and Sugiyama Y (2009) In vitro-in vivo extrapolation of transporter-mediated clearance in the liver and kidney. *Drug Metab Pharmacokinet*. 24:37-52, 2009

Lai L, Tan TM. (2002) Role of glutathione in the multidrug resistance protein 4 (MRP4/ABCC4)-mediated efflux of cAMP and resistance to purine analogues. *Biochem J.* **361**:497-503

Manautou JE, de Waart DR, Kunne C, Zelcer N, Goedken M, Borst P and Elferink RO (2005) Altered disposition of acetaminophen in mice with a disruption of the Mrp3 gene. *Hepatology* **42**:1091-1098.

Matsushima S, Maeda K, Kondo C, Hirano M, Sasaki M, Suzuki H and Sugiyama Y (2005) Identification of the hepatic efflux transporters of organic anions using double-transfected Madin-Darby canine kidney II cells expressing human organic anion-transporting polypeptide 1B1 (OATP1B1)/multidrug resistance-associated protein 2, OATP1B1/multidrug resistance 1, and OATP1B1/breast cancer resistance protein. *J Pharmacol Exp Ther* **314**:1059-1067.

Mizuguchi H and Kay MA (1998) Efficient construction of a recombinant adenovirus vector by an improved in vitro ligation method. *Hum Gene Ther* **9**:2577-2583.

Mizuguchi H and Kay MA (1999) A simple method for constructing E1- and E1/E4-deleted recombinant adenoviral vectors. *Hum Gene Ther* **10**:2013-2017.

Ogilvie BW, Zhang D, Li W, Rodrigues AD, Gipson AE, Holsapple J, Toren P and Parkinson A (2006) Glucuronidation converts gemfibrozil to a potent, metabolism-dependent inhibitor of CYP2C8: implications for drug-drug interactions. *Drug Metab Dispos* **34**:191-197.

Paulusma CC, Bosma PJ, Zaman GJ, Bakker CT, Otter M, Scheffer GL, Scheper RJ, Borst P and Oude Elferink RP (1996) Congenital jaundice in rats with a mutation in a multidrug resistance-associated protein gene. *Science* **271**:1126-1128.

Rius M, Nies AT, Hummel-Eisenbeiss J, Jedlitschky G and Keppler D (2003) Cotransport of reduced glutathione with bile salts by MRP4 (ABCC4) localized to the basolateral hepatocyte membrane. *Hepatology* **38**:374-384.

Rost D, Mahner S, Sugiyama Y and Stremmel W (2002) Expression and localization of the multidrug resistance-associated protein 3 in rat small and large intestine. *Am J Physiol Gastrointest Liver Physiol* **282**:G720-726.

Sasaki M, Suzuki H, Ito K, Abe T and Sugiyama Y (2002) Transcellular transport of organic anions across a double-transfected Madin-Darby canine kidney II cell monolayer expressing both human organic anion-transporting polypeptide (OATP2/SLC21A6) and Multidrug resistance-associated protein 2 (MRP2/ABCC2). *J Biol Chem* **277**:6497-6503.

Shoji T, Suzuki H, Kusuhara H, Watanabe Y, Sakamoto S and Sugiyama Y (2004) ATP-dependent transport of organic anions into isolated basolateral membrane vesicles from rat intestine. *Am J Physiol Gastrointest Liver Physiol* **287**:G749-756.

Suzuki H and Sugiyama Y (1998) Excretion of GSSG and glutathione conjugates mediated by MRP1 and cMOAT/MRP2. *Semin Liver Dis* **18**:359-376.

Ueda K, Kato Y, Komatsu K and Sugiyama Y (2001) Inhibition of biliary excretion of methotrexate by probenecid in rats: quantitative prediction of interaction from in vitro data. *J Pharmacol Exp Ther* **297**:1036-1043.

Watanabe T, Kusuhara H, Maeda K, Shitara Y and Sugiyama Y (2009) Physiologically Based Pharmacokinetic Modeling to Predict Transporter-Mediated Clearance and Distribution of Pravastatin in Humans. *J Pharmacol Exp Ther* **328**:652-662.

Zamek-Gliszczynski MJ, Nezasa K, Tian X, Bridges AS, Lee K, Belinsky MG, Kruh GD and Brouwer KL (2006) Evaluation of the role of multidrug resistance-associated protein (Mrp) 3 and Mrp4 in hepatic basolateral excretion of sulfate and glucuronide metabolites of acetaminophen, 4-methylumbelliferone, and harmol in Abcc3-/- and Abcc4-/- mice. *J Pharmacol Exp Ther* **319**:1485-1491.

Zelcer N, Reid G, Wielinga P, Kuil A, van der Heijden I, Schuetz JD and Borst P (2003) Steroid and bile acid conjugates are substrates of human multidrug-resistance protein (MRP) 4 (ATP-binding cassette C4). *Biochem J* **371**:361-367.

Zelcer N, van de Wetering K, de Waart R, Scheffer GL, Marschall HU, Wielinga PR, Kuil A, Kunne C, Smith A, van der Valk M, Wijnholds J, Elferink RO and Borst P (2006) Mice lacking Mrp3 (Abcc3) have normal bile salt transport, but altered hepatic transport of endogenous glucuronides. *J Hepatol* **44**:768-775.

Zelcer N, van de Wetering K, Hillebrand M, Sarton E, Kuil A, Wielinga PR, Tephly T, Dahan A, Beijnen JH and Borst P (2005) Mice lacking multidrug resistance protein 3 show altered morphine pharmacokinetics and morphine-6-glucuronide antinociception. *Proc Natl Acad Sci U S A* **102**:7274-7279.

Footnote

This study was supported by Grant-in-Aid for Scientific Research (A) from Japan Society for the Promotion of Science (JSPS) (KAKENHI 17209005).

DMD Fast Forward. Published on July 23, 2009 as DOI: 10.1124/dmd.109.027193
This article has not been copyedited and formatted. The final version may differ from this version.

Legends of Figures

Figure 1 Chemical structures of glucuronide conjugates used in this study

Figure 2 Plasma concentration profiles of glucuronide conjugates in wild-type and *Mrp3*$^{-/-}$ mice.

Wild-type (closed circle) and *Mrp3*$^{-/-}$ mice (open circles) received oral doses of gemfibrozil (20 mg/kg), E3040 (2 mg/kg), troglitazone (25 mg/kg), bisphenol A (10 mg/kg) and 4-methylumbelliferon (18 mg/kg). The plasma concentrations of Gem-G (panel a), E3040G (panel b), TGZ-G (panel c), BisA-G (panel d) and 4-MUG (panel e) were determined at the indicated time points (n =3 - 5 per time point). *$p < 0.05$, **$p < 0.01$ wild-type versus *Mrp3*$^{-/-}$ mice.

Figure 3 Uptake of glucuronide conjugates by MRP2-, MRP3- and MRP4-expressing membrane vesicles in the presence of ATP or AMP.

Uptake of [^{3}H]$E_2$17βG (a), Gem-G (b), E3040G (c) and TGZ-G (d) was measured in isolated membrane vesicles prepared from LLC-PK1 cells expressing MRP2, HEK293 cells expressing MRP3 and HEK293 cells expressing MRP4. Membrane vesicles were incubated at 37 °C with [^{3}H] $E_2$17βG (300 nM), Gem-G (25μM), E3040G (500 nM) and TGZ-G (10 μM), in the presence of ATP (■) or AMP (□) for 2min. Data represent mean values ± S.E. of three independent determinations. * $p<0.05$, ** $p<0.01$ (mock control *versus* MRP2) † $p<0.05$, †† $p<0.01$ (mock control *versus* MRP3 or MRP4)

Figure 4 Western blots of human OATP1B1, MRP2 and either MRP3 or MRP4 in triple transfectants.

(a) Cell lysate (15 µg) from MDCK II control cells (lane 1), OATP1B1/MRP2 double transfectant (lane 2) and OATP1B1/MRP2/MRP3 triple transfectant (lane 3) and OATP1B1/MRP2/MRP4 triple transfectant (lane 4) were subjected to SDS-PAGE polyacrylamide gel electrophoresis (8.5 % acrylamide separating gel). OATP1B1 and MRP4 were detected with their respective polyclonal antibodies and MRP2 and MRP4 were detected by their respective monoclonal antibodies. **(b)** Cell lysate from MRP3 or MRP4 triple transfectants (5 µg, lane 1) and crude membrane from human liver (20 µg, lane 2 and 3) were subjected to SDS-PAGE polyacrylamide gel electrophoresis (8.5 % acrylamide separating gel). MRP3 and MRP4 were detected by their respective polyclonal and monoclonal antibodies, respectively.

Figure 5 Membrane Localization of human MRP3 and MRP4 in transfected MDCK II cells.

MDCK II double transfectants that were infected with MRP3 (a) or MRP4 (b) recombinant adenovirus were stained with polyclonal antiserum against human MRP3 (green fluorescence) and monoclonal antibodies against human MRP2 (red fluorescence) and human MRP4 (green fluorescence). Nuclei were stained with TO-PRO-3 (blue fluorescence). Pictures are single optical sections (X/Y) (center) with X/Z (top) and Y/Z (right) projections, respectively. Horizontal sections are at positions indicated by arrow-heads in X/Z (top) and X/Z (right) projections, and vertical sections through the cell monolayers are at positions indicated by arrow-heads in X/Y sections (center).

Figure 6 Time-profiles for the transcellular transport of glucuronide conjugates in control,

DMD Fast Forward. Published on July 23, 2009 as DOI: 10.1124/dmd.109.027193
This article has not been copyedited and formatted. The final version may differ from this version.

OATP1B1/MRP2 double transfectant, OATP1B1/MRP2/MRP3 and OATP1B1/MRP2/MRP4 triple transfectants

Transcellular transport of [^{3}H] $E_2$17βG (0.3 μM, panel a), Gem-G (5 μM, panel b), E3040G (0.5 μM, panel c) and TGZ-G (10 μM, panel d) across the monolayers of control MDCK II (left), OATP1B1/MRP2 double transfected, OATP1B1/MRP2/MRP3 triple transfected (middle) and OATP1B1/MRP2/MRP4 triple transfectants (right) was determined. The experiments were performed three times in triplex, and reproducibility was confirmed. The representative data are shown in the graphs. Open and closed circles represent the transcellular transport in the basal-to-apical and apical-to-basal direction in control cells. Open squares and diamonds represents the transcellular transport in the basal-to-apical and apical-to-basal direction in OATP1B1/MRP2 double transfectant (middle and right). Closed squares and diamonds represents the transcellular transport in the basal-to-apical and apical-to-basal direction in MRP3 and MRP4 triple transfectants (middle and right, respectively). Points and vertical bars represent the mean ± S.E. of three independent determinations. Where vertical bars are not shown, the S.E. was contained within the limits of the symbol. * $p<0.05$, ** $p<0.01$ (double versus triple transfectants)

Table 1. LC/MS conditions for the quantification of the non-radioactive compounds.

compound	column	mobile phase		Gradient condition		flow rate	desolvation	capillary	cone	M/Z	Ion
		A	B	time (min)	A/B	(ml/min)	temp (ºC)	vol. (V)	volt. (V)		mode
4-MU	L-column ODS,	0.05% formic acid	acetonitrile	0	85/15				25	175	-
4-MUS	5µm,			1.5	30/70	0.3	350	3.2	25	225	-
4-MUG	2.1×150mm			1.51	85/15				25	351	-
Bisphenol A	CAPCELL PAK	0.01 M	acetonitrile	0	85/15				40	227	-
Bis-AG	C18 MGII, 3µm,	ammoniumu		1.5	30/70	0.4	350	3.2	25	403	-
	2×50mm	acetate (pH6)		1.51	85/15						
E3040	CAPCELL PAK	0.01 M	acetonitrile	0	85/15				40	300	+
E3040G	C18 MGII, 3µm,	ammoniumu		3	20/80	0.4	350	3.2	25	380	+
E3040S	2×50mm	acetate (pH6)		3.01	85/15				40	476	+
gemfibrozil	CAPCELL PAK	0.01 M	acetonitrile	0	85/15				17.5	249.1	-
Gem-G	C18 MGII, 3µm,	ammoniumu		3	20/80	0.4	350	3.2	20	424.9	-
	2×50mm	acetate (pH6)		3.01	85/15						
troglitazone	CAPCELL PAK	0.01 M	acetonitrile	0	85/15				40	440	-
TGZ-S	C18 MGII, 3µm,	ammoniumu		3	20/80	0.4	350	3.2	30	520	-
TGZ-G	2×50mm	acetate (pH6)		3.01	85/15				30	616	-

Abbreviations: 4-MU, 4-methylumbelliferone; 4-MUS, 4-MU sulfate; 4-MUG, 4-MU glucuronide; Bis-AG, bispheol-A glucuronide; E3040, 6-hydroxy-5,7-dimethyl-2-methylamino-4-(3-pyridymethyl)benzothiazole; E3040G, E3040 glucuronide; E3040S, E3040 sulfate; Gem-G, gemfibrozil 1-*O*-β-glucuronide; TGZ-G, troglitazone glucuronide; TGZ-S, troglitazone sulfate

Table 2 The area under the curve of the plasma concentration time profiles of parent durgs and their glucuronide conjugates in wild-type and *Mrp3*$^{-/-}$ mice

Mice received oral doses of gemfibrozil (20 mg/kg), E3040 (2 mg/kg), troglitazone (25 mg/kg), bisphenol A (10 mg/kg) and 4-methylumbelliferone (18 mg/kg). The area under the plasma concentration time curve of the parent compounds and their glucuronide conjugates were obtained by trapezoidal rule.

	$AUC_{0\rightarrow\infty}$ (nmol•min/ml)									
	gemfibrozil		E3040		troglitazone		bisphenol A		4-MU	
	gemfibrozil	Gem-G	E3040	E3040G	troglitazone	TGZ-G	bisphenol-A	Bis-AG	4-MU	4-MUG
wild-type	3330±90	1500±200	0.174±0.030	11.7±5.3	323±60	246±6	ND	620±133	ND	2990±600
Mrp3$^{-/-}$	3020±140	431±13**	0.384±0.110	0.500±0.120**	687±181	ND	ND	61.7±10.0**	ND	753±118**

Abbreviations: GEM-G, gemfibrozil 1-*O*-β-glucuronide; E3040, 6-hydroxy-5,7-dimethyl-2-methylamino-4-(3-pyridymethyl)benzothiazole; E3040G, E3040 glucuronide; E3040S, E3040 sulfate; TGZ-G, troglitazone glucuronide; Bis-AG, bisphenol-A glucuronide; 4-MU, 4-methylumbelliferone; 4-MUG, 4-MU glucuronide; ND, not detected

Fig. 1

gemfibrozil glucuronide

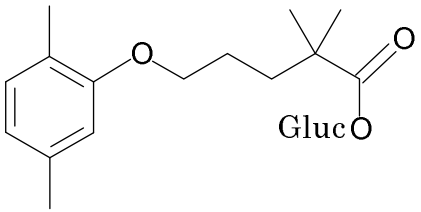

bisphenol A glucuronide

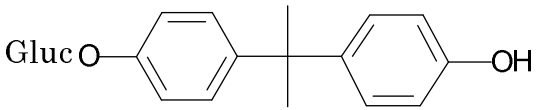

E3040 glucuronide

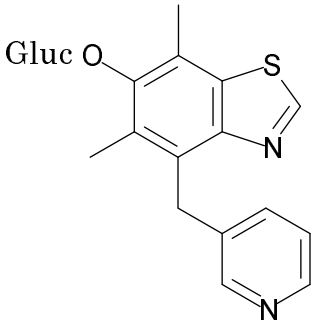

4-methylumbelliferone-glucuronide

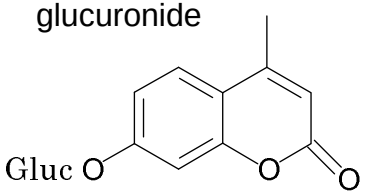

troglitazone-glucuronide

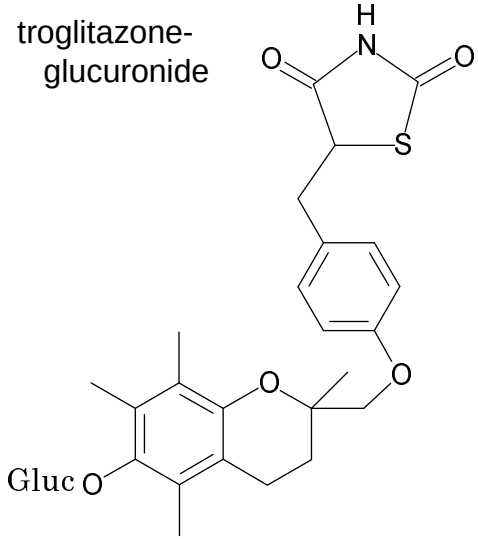

Fig. 2

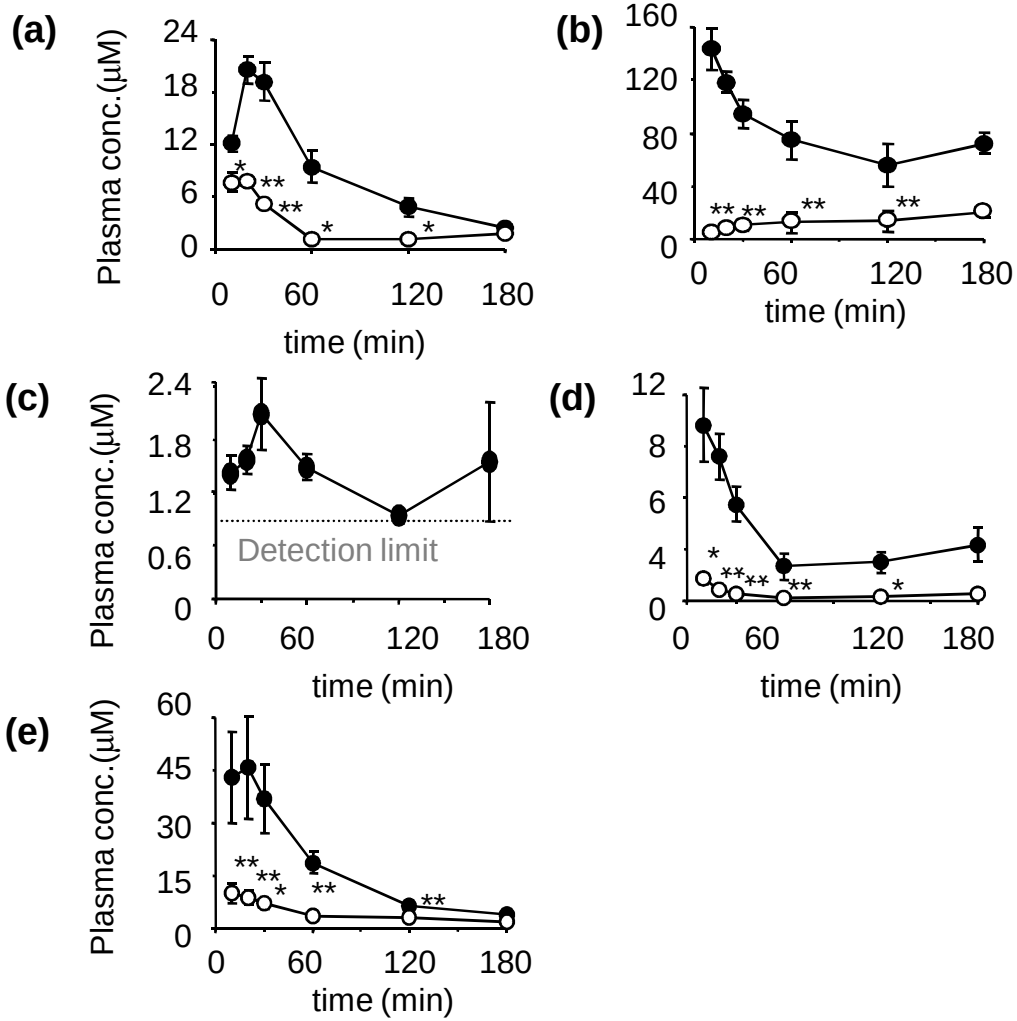

Fig. 3

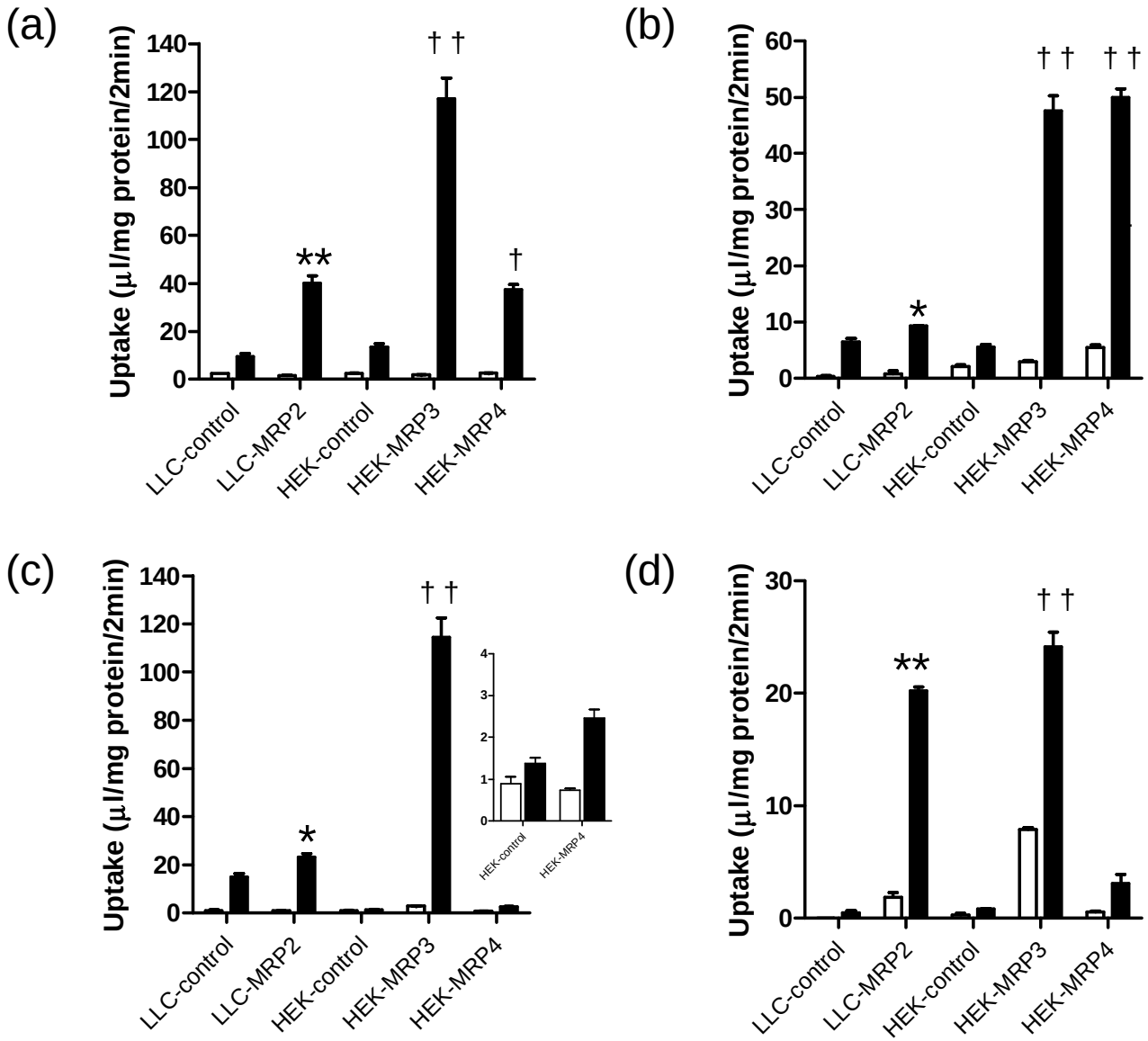

Fig. 4

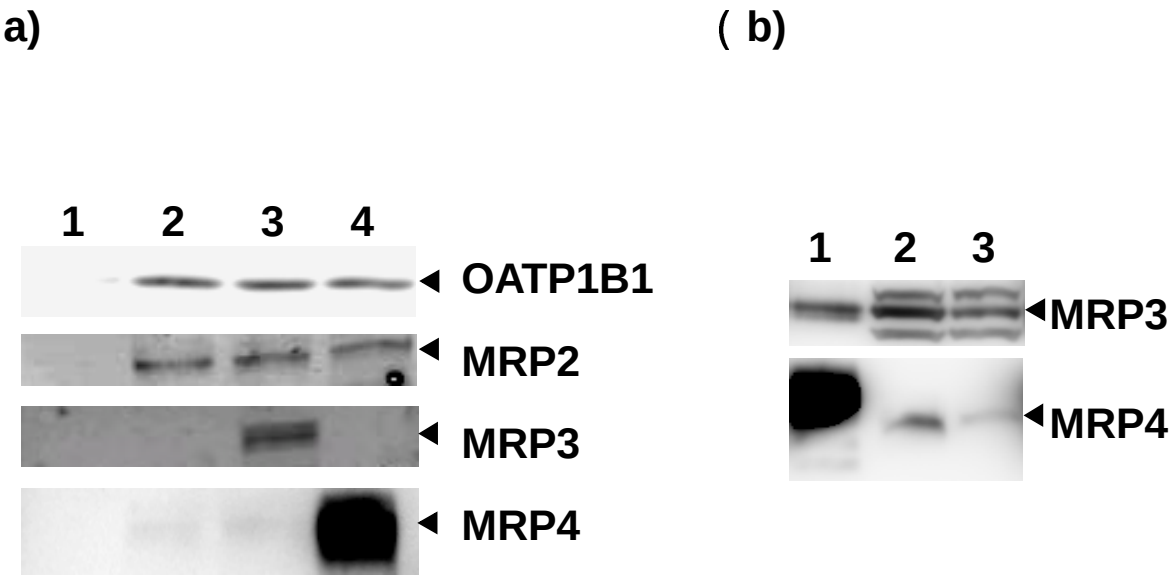

Fig. 5

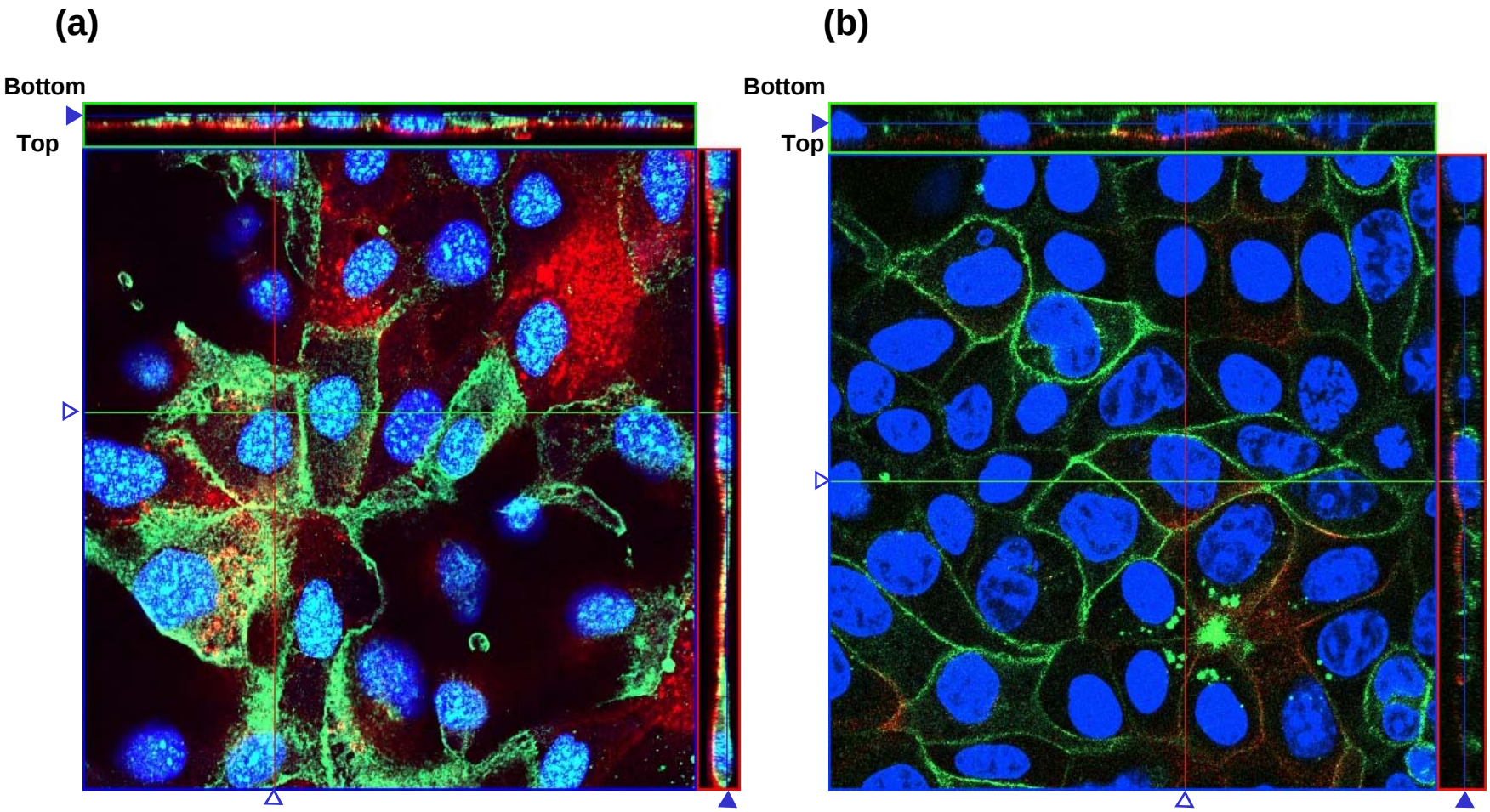

DMD Fast Forward. Published on July 23, 2009 as DOI: 10.1124/dmd.109.027193
This article has not been copyedited and formatted. The final version may differ from this version.

Fig.6